

Patch microstructure in cement-based materials: Fact or artefact?

H.S. Wong *, N.R. Buenfeld

Concrete Durability Group, Department of Civil and Environmental Engineering, Imperial College London, SW7 2AZ, UK

Received 9 March 2005; accepted 9 February 2006

Abstract

The appearance of patch microstructure, i.e. broad dense and porous regions separated by sharp and distinct boundaries and occurring randomly in bulk and interfacial transition zones, has been reported previously in various site- and laboratory-mixed concretes and mortars. In this paper, evidence is presented to show that patch microstructure is an artefact of sample preparation and does not reflect the true nature of the hydrated cement paste. The appearance of dense patches comes from paste areas that have been ground and polished beyond the epoxy resin intrusion depth. In a backscattered electron image, pores not filled with epoxy are not visible because the signal is generated from the base or side walls of the pores. A modified method for epoxy impregnation, which can achieve a much deeper epoxy penetration than conventional vacuum impregnation, is presented.

© 2006 Elsevier Ltd. All rights reserved.

Keywords: Backscattered electron imaging (B); Image analysis (B); Interfacial transition zone (B); Microstructure (B); SEM (B); Percolation

1. Introduction

Patch microstructure was first reported in this journal [1] in an experimental investigation using backscattered electron (BSE) microscopy in the context of the phenomenon of percolation due to overlapping of interfacial transition zones (ITZs) in mortar. Further reports on patch microstructure by the same author have since appeared elsewhere [2–4]. The original paper [1] claimed to invalidate the conclusion of Winslow et al. [5] that the mercury intrusion porosimetry results, which showed increased intruded pore space at pressures below the threshold pressure in mortars with sand contents of at least 48%, can be attributed to percolation of overlapping porous ITZs. Diamond [1] made the following observations:

- The hardened cement paste in mortars (w/c ratio 0.4, 28 days old, sand volume fraction >48 vol.%) consists of ‘patches of brighter, dense, almost nonporous regions and dark, highly porous patches; the patches indifferently occupying both classical ‘ITZ’ and classical ‘bulk’ locations’.
- Dense and porous patches ‘do not blend together, but form sharp boundaries’.

- The porous regions occur in broad patches through the bulk paste. Many sand particles are ‘surrounded or partly surrounded by the dense, almost non-porous hardened cement paste’. This is inconsistent with the conventional ITZ model.
- The proportion of porous patches increases with sand content and, at high (48.6 vol.%) sand contents, the porous patches are ‘visibly interconnected on the plane of observation’.

From the above observations, Diamond [1] concluded that if percolation occurs in high sand content mortars, the percolative effect is a result of the interconnection of highly porous patches and not from the overlapping of ITZs [6]. In another paper, Diamond [2] found similar porous and dense patches in site- and laboratory-mixed concretes of 0.45 w/c ratio. More recently, Diamond [4] showed that this distinctive patchy microstructure is not a result of inadequate mixing. The dense and porous patches persisted despite prolonged mixing of up to 30 min.

We have made similar observations (unpublished) of patch microstructure, in our routine work using backscattered electron imaging. An example is shown in Fig. 1, which is a BSE image of a mortar (w/c 0.6, sand 50 vol.%, 28 days sealed cured) that has been vacuum impregnated with epoxy, then ground and polished using conventional methods. As can be seen in the figure, the

* Corresponding author. Tel.: +44 20 7594 5957; fax: +44 20 7225 2716.
E-mail address: hong.wong@imperial.ac.uk (H.S. Wong).

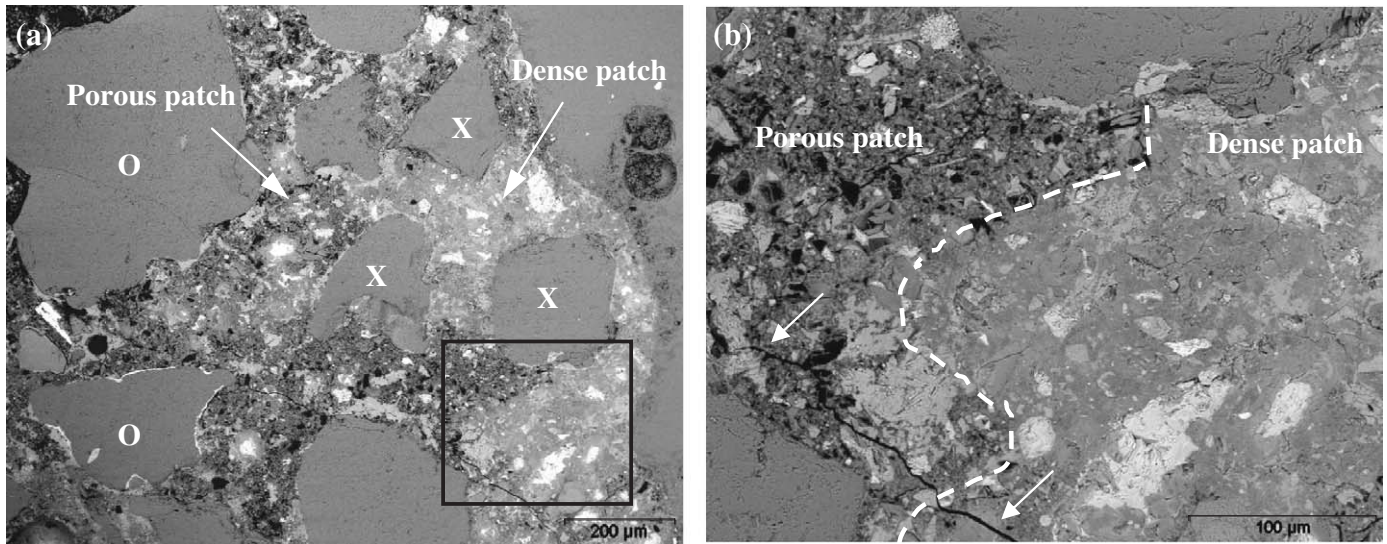


Fig. 1. (a) Patch microstructure observed on an OPC mortar (w/c 0.6, sand 50 vol.%, 28-day cured) where dark porous cement paste appears to be intermixed with bright, almost non-porous paste. Particles marked 'O' represent sand particles that are fully surrounded by porous cement paste while particles marked 'X' are in contact with both porous and dense patches. Field of view is $1333 \times 1000 \mu\text{m}$. (b) Magnified portion of (a) showing the boundary between the porous and dense patch is sharp and distinct. Field of view is $381 \times 286 \mu\text{m}$.

cement paste appears to consist of two distinct types of hardened cement paste. One appears dark and porous while the other appears relatively bright, dense and almost non-porous. The dense/porous patches often extend to several hundreds of microns in width, occur indiscriminately in both ITZ and bulk paste regions and do not seem to be influenced by the size, orientation and spatial distribution of the aggregate particles. Some aggregate particles are completely surrounded by porous paste while others are in contact with both the porous and dense pastes.

The most remarkable feature is the boundary between the dense and porous patches, which is unusually distinct and sharp. In Fig. 1(b), the paste on the left appears very porous with interconnected capillary pores and hollow shells. In contrast, the paste on the right appears almost non-porous with several unreacted cement grains visible, surrounded by very dense hydration products. A continuous microcrack can be seen on the bottom left of the image (indicated with an arrow), extending between the dense and porous patches. It should be noted that the patch microstructure shown here is very similar to those reported previously (see, for example, Figs. 1, 4 and 10 of Diamond [1]). In this paper, we shall provide evidence that such patch microstructure, in particular where a sharp boundary is present, is an artefact of specimen preparation and does not reflect the true nature of the cement paste.

2. Epoxy impregnation

For microstructural examination of porous media using backscattered electron microscopy, it is essential for the pores to be first saturated with epoxy resin, which upon hardening, supports the delicate pore structure and enables it to withstand subsequent grinding and polishing with minimal induced damage. The epoxy also serves a second, but equally important, purpose; due to its low average atomic number, the epoxy allows the pores to be visible and be differentiated from solid

phases during BSE imaging. When the microscope electron beam is directed onto a pore that is not resin-filled, the incident electrons will continue to travel below the observation plane until they hit a solid material, which is either the base or side wall of the pore. The incident electrons will interact with the solid phase and after a series of scattering events, may re-emerge as backscattered electrons, escape the empty pore and be collected by the detector. In the resulting BSE image, the corresponding 'pore' pixel will then appear bright, depending on the average atomic number of the solid phase that surrounds the pore. Unfortunately this phenomenon is often overlooked.

The general procedure for conventional epoxy impregnation is briefly described here. The sample is first dried either by oven drying, vacuum drying, freeze-drying after immersion in liquid nitrogen, or by solvent replacement which takes a longer time. Removal of water from the pore channels is essential because it interferes with the penetration and polymerisation of the epoxy. The dried sample is then fitted into a casting mould and evacuated in a vacuum chamber. The epoxy, preferably de-aired, is fed into the mould whilst still under vacuum until the sample is completely submerged. The epoxy and sample are allowed to out-gas, and after some time, the vacuum is slowly released to allow air in, which theoretically pushes the epoxy into the pores. In reality, the intrusion depth achieved by this method is very small, because the pores in most cement-based materials are very fine, and this is well known [7,8]. For example, Kjellsen et al. [7] showed that the epoxy penetration depth for a 0.4 w/c ratio paste was only around $120 \mu\text{m}$ and this decreased with decreasing w/c ratio and the presence of silica fume.

Obviously, grinding and polishing should not go beyond the epoxy intrusion depth, but this is extremely difficult with such a shallow epoxy penetration. Also, in the first stage of dry grinding, silicon carbide papers of a very coarse grit size, typically 100–150 grit (90–160 μm grain diameter) [7,9] are used to remove excess resin from the sample surface, and thus, this stage has to be

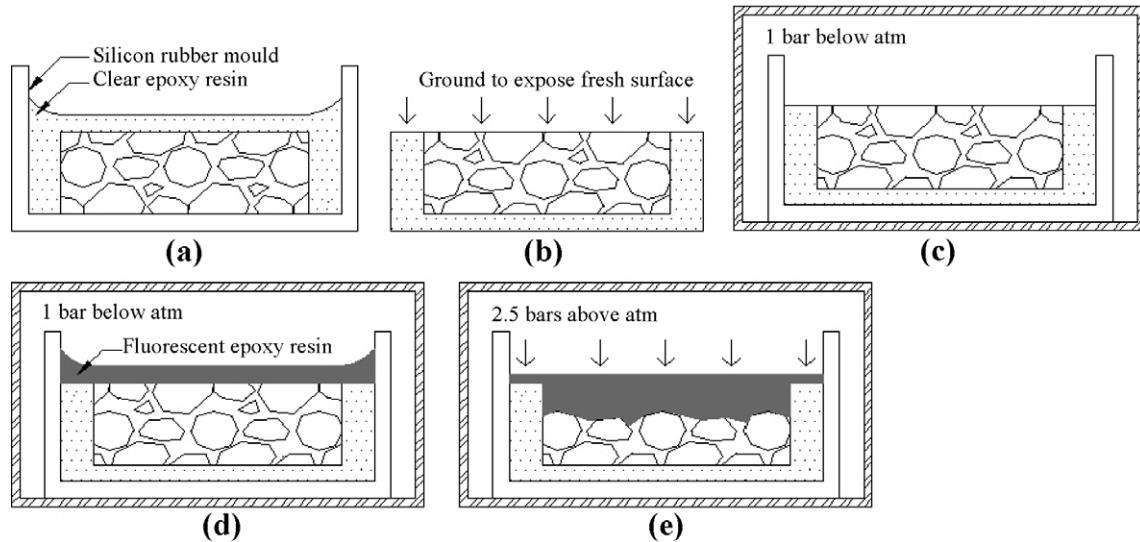


Fig. 2. Schematic of the new epoxy impregnation method: (a) the dried sample is first cast in clear epoxy resin; (b) when the resin has hardened, the bottom face is dry-ground to expose a fresh and plane surface for observation; (c) the sample is placed under vacuum for several hours to evacuate the pores; (d) a de-aired fluorescent epoxy resin is added while the sample is still under vacuum; (e) and finally the vacuum is released and a 2.5 bars gas pressure is applied for 30 min.

controlled with extreme care. The difficulty is compounded by the uneven thickness of the surplus resin, uneven rate of material removal during grinding (the sample edge is usually ground faster than its centre) and surface roughness from previous cutting operations that must be removed in order to achieve a plane section. If the coarse grinding stage is not done sufficiently, so as to reveal the epoxy-filled surface, then many large and irregularly shaped pockets of black resin-filled voids will be seen in the BSE images, giving a false impression of a very porous, poorly consolidated sample. In addition, it is very difficult to tell if the sample remains saturated with epoxy after the polishing stages unless a coloured dye is added into the epoxy.

We have developed a slight modification to the resin impregnation procedure to achieve deeper epoxy penetration. The steps are illustrated in Fig. 2. First, the dried sample is cast in a clear epoxy resin with the observation plane at the bottom.

When the resin has achieved sufficient hardness, the sample is dry ground to remove the excess clear resin and to expose a fresh, planar surface. Then, compressed air is used to dislodge any grinding material or dirt from the surface. Next, the sample is placed under vacuum for 4 h; this is important to ensure that the pores are completely de-aired. Without breaking the vacuum, a low viscosity fluorescent resin (araldite) that has been previously de-aired and diluted with 5 wt.% toluene (to reduce viscosity further) is poured onto the sample, covering the entire surface. The vacuum is released and subsequently, an additional 2.5 bars above atmospheric pressure is applied on the sample via a gas (O_2) bottle, and maintained for about 30 min. Pressuring the sample at this level is routinely used in gaseous permeability testing and is not known to cause damage. Fig. 3 shows parallel mortar samples that were impregnated using the conventional vacuum technique (A and B) and the new method

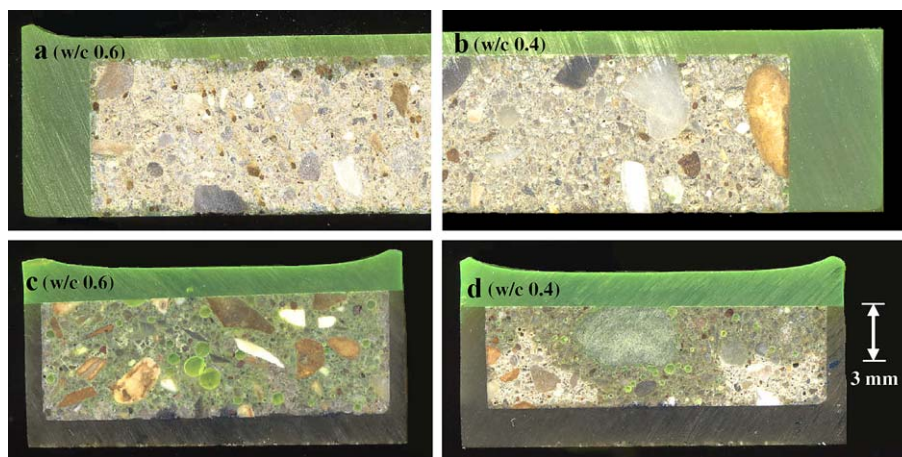


Fig. 3. Cross sections of mortar samples showing the depth of resin penetration using the conventional vacuum impregnation method (A, B) and the new technique (C, D). The epoxy penetration front is less than 1 mm on samples that were impregnated using the conventional method. Full depth penetration is evident for the w/c 0.6 mortar (C) and a penetration of around 3 mm for the w/c 0.4 mortar (D). The deeper epoxy penetration provides confidence that the observation plane remains saturated with epoxy after the grinding and polishing stages.

(C and D). The difference in penetration depth is clear. Whilst the epoxy penetration front is less than 1 mm on the vacuum impregnated samples, a full (7 mm) depth of penetration was achieved for the 0.6 w/c ratio mortar specimen and approximately 3 mm penetration was achieved for the 0.4 w/c ratio mortar when the new method was used. However, we note that although the new method achieves a deeper penetration depth, it does not necessarily imply that all capillary pores have been filled with epoxy to that depth. Nevertheless, a greater epoxy penetration depth gives more tolerance during the grinding stages and ensures that the observation plane remains filled with epoxy after polishing.

3. Experimental

Two mortars with w/c ratios of 0.4 and 0.6 were prepared using ordinary Portland cement and medium graded siliceous sand at 50 vol.% fraction. A conventional pan mixer was used. The sand and cement were dry-mixed for 2 min and then water was added as the mixer continued to rotate. The total wet mixing time was 3 min. The mortars were cast in steel cylindrical moulds (100 \varnothing × 250 mm) and compacted in three uniform layers using a vibrating table. After 24 h, the samples were demoulded, sealed in cling film and cured at 20 °C for 28 days. At the end of the curing period, an 8 mm thick disc was cut from each cylinder at approximately 125 mm from the bottom cast face, from which a block specimen (40 × 20 × 8 mm³) was extracted. Cutting was performed using a precision diamond saw and a non-aqueous lubricant. The blocks were freeze-dried using liquid nitrogen and vacuum-impregnated with a low viscosity epoxy following the conventional procedure described in the previous section. The block samples were then dry-ground using silicon carbide papers of successively finer grit size (120, 220, 500, 1000 and 1200) and finally polished using cloths embedded with diamond abrasives (9, 6, 3, 1 and 0.25 μ m) with a non-

aqueous lubricant. Each grinding and polishing step was done at 70 rpm and 7 N applied force. Polishing time was kept short (~5 min) to minimise relief. The sample was cleaned ultrasonically in acetone after each polishing stage.

A JEOL 5410LV scanning electron microscope equipped with a backscatter electron detector was used for imaging. The microscope was operated at low vacuum (9 Pa), hence carbon coating was not necessary, 10 kV accelerating voltage and 10 mm free working distance. The images were digitised to 1024 × 768 pixels. Each image was captured with a constant brightness and contrast settings for reproducibility. The brightness and contrast were adjusted so that the greyscale histogram of the image was stretched to cover the entire greyscale spectrum, but was not over-saturated at the low or high ends of the spectrum. However, it was observed that the lens current tended to fluctuate even after a long warm-up time and hence, the brightness and contrast settings were checked and readjusted periodically. The brightness and contrast were calibrated with an aluminium–epoxy microanalytical standard prior to the capture of each image.

Areas that showed patchy microstructure were imaged at several magnifications. The co-ordinates of these locations were stored so that they could be revisited later. In total, ten locations were chosen per sample. The samples were then re-impregnated with epoxy using the proposed technique, but without the initial grinding stage (Fig. 2b). After that, the samples were ground and polished according to the same procedure as described above. The locations that initially showed patchy appearance were revisited in the electron microscope to establish if the dense/porous patches persisted.

4. Observations

In all the locations that we re-examined, it was found that the dense patches disappeared after the samples were re-

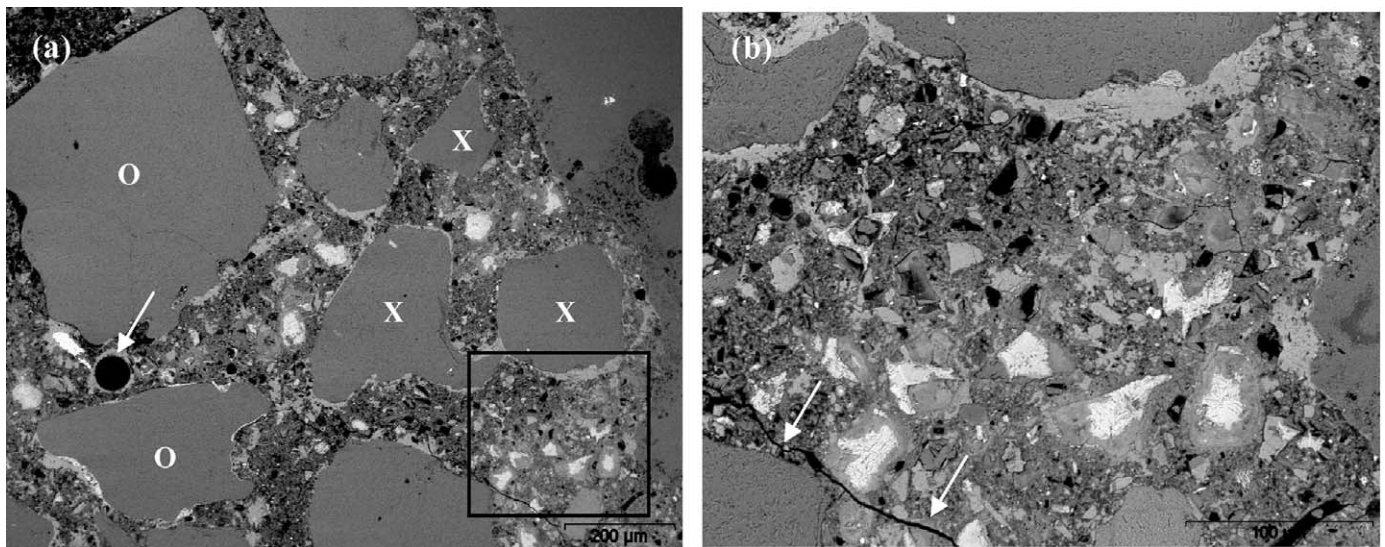


Fig. 4. Area matching BSE images of those shown in Fig. 1, after re-impregnation and re-polishing. The originally dense patches are now filled with capillary pores and hollow shell pores that were previously unseen. By monitoring the change in diameter of the spherical air void (indicated with an arrow in (a)), the amount of material that has been removed from the re-grinding and re-polishing is estimated to be around 50 μ m. The microcrack (indicated with arrows in (b)) is also visible in Fig. 1b.

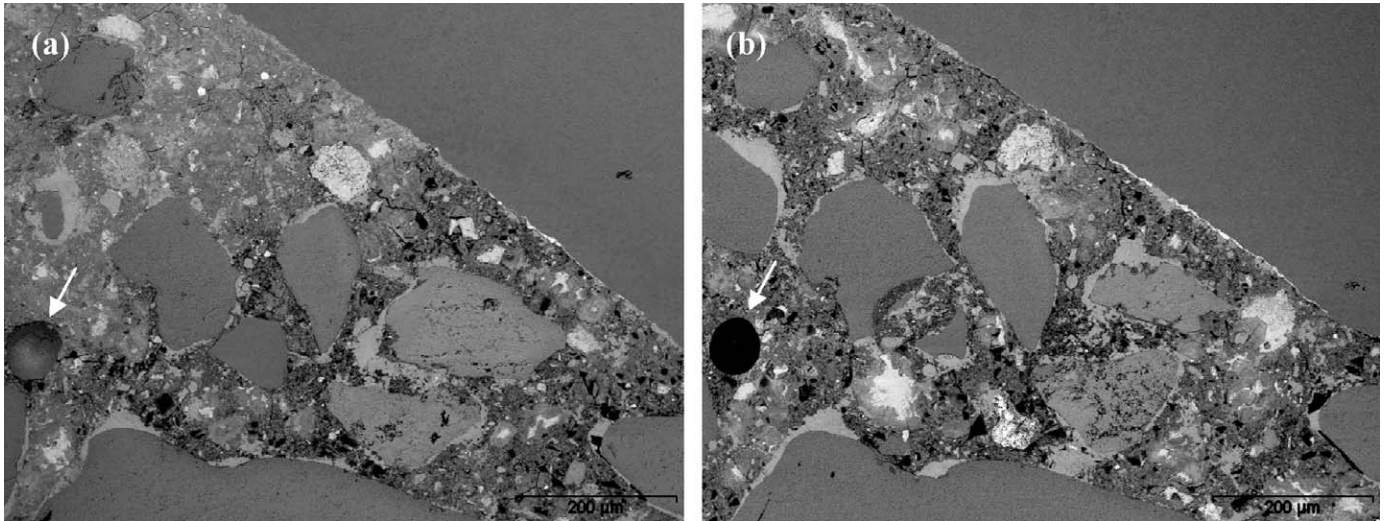


Fig. 5. Area matching images of before (a) and after (b) epoxy re-impregnation. In (a), the large sand particle at the top right corner was originally in contact with both dense and porous patches. An empty air void can also be seen (arrowed) in the dense patch (w/c ratio 0.4, field of view: $889 \times 667 \mu\text{m}$).

impregnated and re-polished. Fig. 4 shows BSE images of the same area as the one in Fig. 1 after having been re-impregnated and re-polished. By measuring the change in diameter of the air void (indicated by an arrow in Fig. 4a), and by assuming that it follows a spherical shape, it is estimated that the thickness of material that had been removed during the second grinding/polishing stage was around $50 \mu\text{m}$. It is clear from Fig. 4 that the apparently dense patches that were visible in Fig. 1 have now disappeared. The originally dense patches are now filled with many capillary pores and hollow shell pores. The same microcrack can be seen in Figs. 1b and 4b, suggesting that the crack runs deep into the sample and was more easily penetrated by epoxy than the fine capillary pores. This probably explains why the crack was visible in the dense patch of Fig. 1b.

Fig. 5(a) shows a large sand particle in the top right corner that is in contact with both dense and porous patches, giving a false impression concerning the nature of the interfacial transition zone. In the same image, an empty air void (arrowed) is located in the dense patch. The edge of the void appears darker than the centre because near the edge, some of the emitted backscattered electrons from the bottom will hit the side walls and re-penetrate the sample. These re-entry electrons are of much lower energy than incident electrons and are unlikely to escape again as backscattered electrons. However, this pore edge darkening effect will be less obvious in smaller voids such as capillary pores and hollow shells. Therefore, empty (i.e. not filled with epoxy) capillary pores and hollow shells will have a similar intensity to the surrounding solid phase, and appear like a dense mass of hydration products and unreacted cement

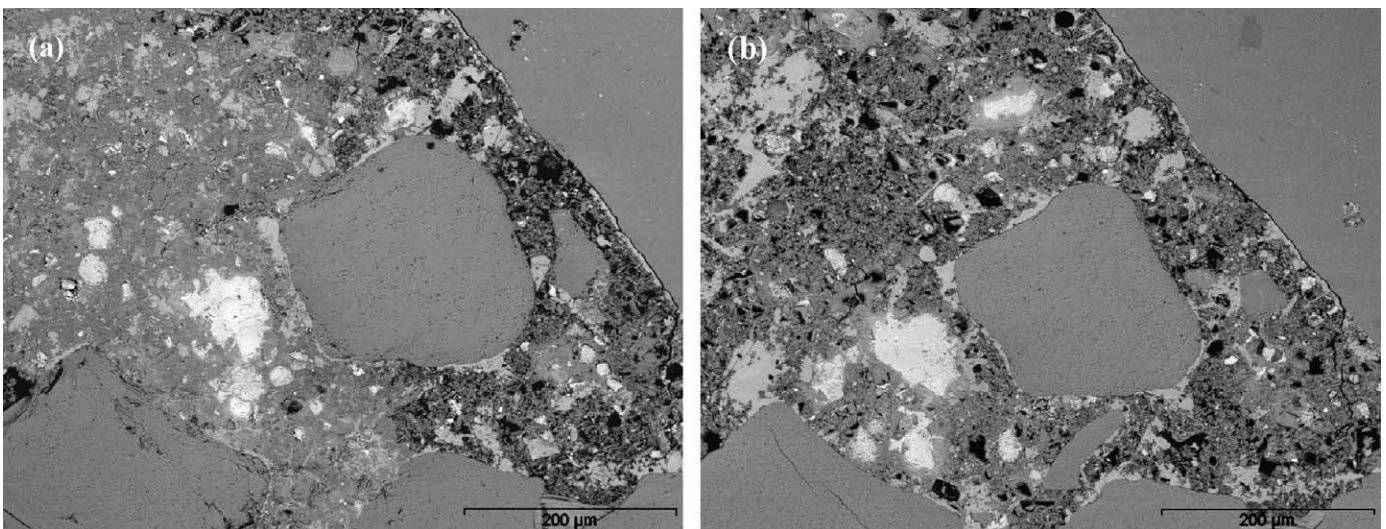


Fig. 6. Area matching images of before (a) and after (b) epoxy re-impregnation. Image (a) gives a false impression that the sand particle at the top right corner is surrounded by a very porous ITZ (w/c ratio 0.6, field of view: $667 \times 500 \mu\text{m}$).

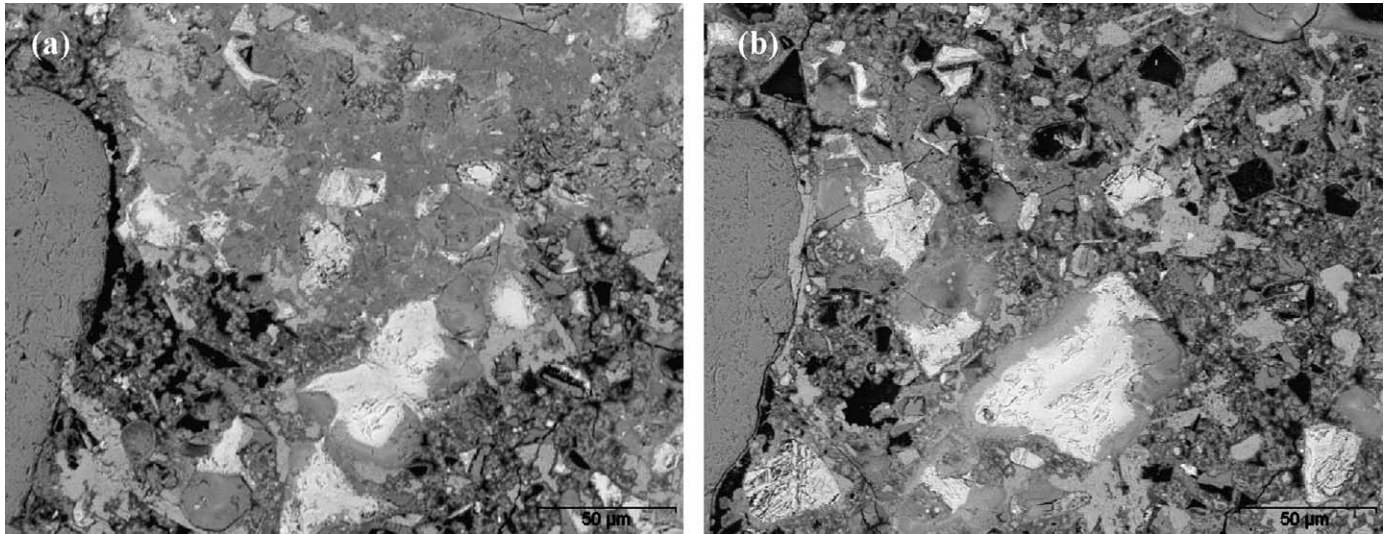


Fig. 7. Higher magnification image of a sharp boundary between a dense and a porous patch (a) which disappears after re-impregnation (b) (w/c ratio 0.6, field of view: $267 \times 200 \mu\text{m}$).

grains. In Fig. 5b, when the sample is properly saturated with resin, the paste is more homogeneous and the same air void is completely black.

Fig. 6(a) shows a sand particle at the top right corner that is apparently surrounded by a very porous ITZ. Quantitative image analysis, i.e. strip analysis, performed on this particle would most certainly lead to a false conclusion. In Fig. 6(b), after the sample is re-impregnated, the paste is more homogeneous with no clear indication of a porous ITZ. Figs. 7 and 8 show higher magnification images of areas that originally had a sharp and almost linear boundary between the porous and the dense patches. After epoxy re-impregnation, the sharp boundary disappears and more pore features are visible in the 'dense patch'. In Fig. 8b, the paste region between the two closely spaced sand particles appears to be

more porous than the paste region farther away from the aggregate surface, perhaps suggesting the ITZ phenomenon.

5. Discussion

It might be argued that the unique specimen preparation procedure applied in this study has somehow altered the nature of the pore structure. The small amount of toluene, which was added to the epoxy to lower its viscosity, is not known to have any dissolving action on cement hydration products. Samples were not ground prior to the second epoxy impregnation. Thus if the dense patches are real features, the epoxy should not be able to penetrate into the sample during the second impregnation. The higher pressure may force the epoxy into the dense patches, but if this were the case, then the originally dense

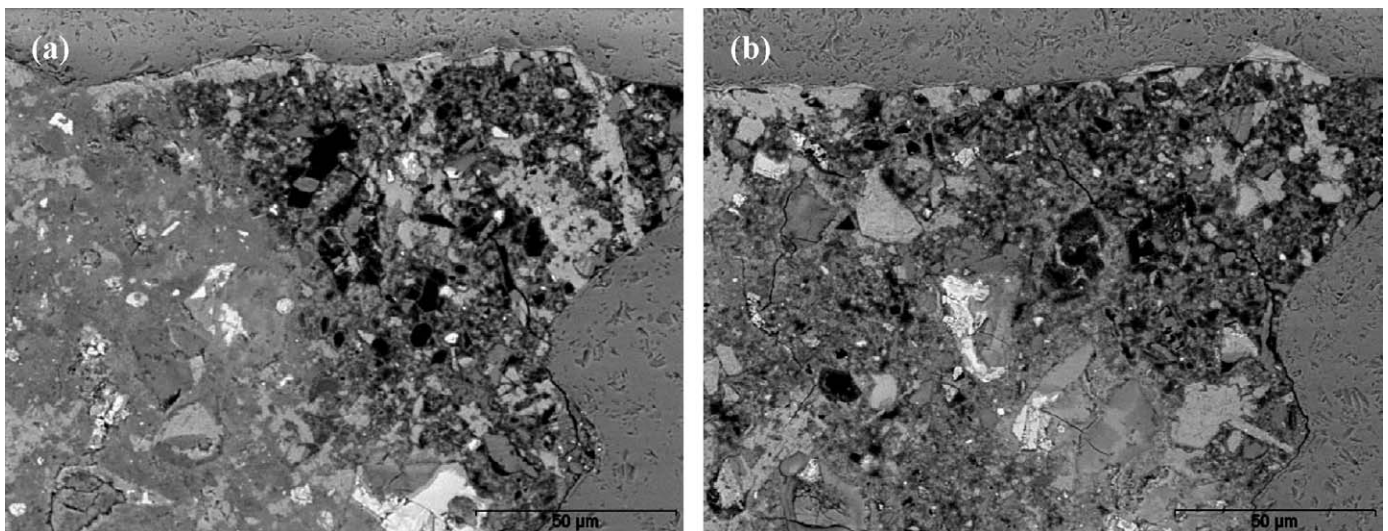


Fig. 8. Higher magnification image of a sharp boundary between a dense and a porous patch (a) which disappears after re-impregnation (b). The paste region between the two closely spaced sand particles appears more porous than the bulk paste, suggesting the ITZ effect (w/c ratio 0.4, field of view: $178 \times 133 \mu\text{m}$).

patches should re-appear as pastes with much finer capillary pores compared to the originally porous patches.

Re-grinding and re-polishing the sample inevitably removes some material and therefore the second image is not of exactly the same area as the first. However, the layers that were removed were only very thin, because the samples were already planar. Many features such as sand particles, cracks and large cement grains that were in the first image could still be seen in the second image. It might be argued that re-grinding discarded the dense patches, exposing an underlying porous patch in the second image. If this were true, then the reverse would also be expected, i.e. a porous patch being replaced by a dense patch, yet we have not seen such an occurrence in any of the images that were examined.

The capillary pores and hollow shells observed appear to be typical of those normally seen in a BSE image and do not appear to be artefacts. In fact, the re-polished samples were found to have significantly fewer microcracks and less preparation damage compared to the initial sample with dense/porous patches. All the locations that were initially marked showing patchy microstructure have produced a similar change upon re-impregnation. A random search on the re-impregnated samples failed to locate any more of the dense patches. Therefore, we are convinced that the second set of images shown here is representative of the true microstructure and is not the result of a series of coincidences.

If the patchy appearance reported in previous publications and reproduced in this paper is indeed an artefact of specimen preparation, it then raises the question of the validity of quantitative image analysis results that have been published on the ITZ phenomena by the same author [10,11]. These investigations found that the detectable porosity of cement paste in the ITZ differs on average, only slightly from the cement paste in the bulk regions and that the spatial distribution of detectable pores was highly irregular. It was observed that porous patches and relatively dense patches intermingled irregularly in both bulk and ITZ regions, which led the authors [10,11] to doubt the conventional picture of the ITZ. Unfortunately, not much information was provided on the sample preparation procedure, except that in Diamond [1], it was mentioned that the sample preparation was carried out at the laboratories of R.J. Lee Group, which involved 'gentle drying', impregnation of very low viscosity epoxy resin under vacuum, followed by the 'usual' grinding, polishing and carbon coating procedures. This information alone, however, is insufficient to gauge if the samples have been ground beyond the epoxy penetration depth.

This study has also raised other issues. Since pores are only visible when they are resin-filled, it makes one wonder whether the appearance of dense paste in mature or high-performance concretes is really due to lack of capillary pores, or because the pores are too fine to be impregnated by the epoxy resin. Related to this is the issue of whether the smallest detectable pore in a BSE image is controlled by the resolving power of the imaging system, or, limited by the ability of the epoxy resin to penetrate fine capillary pores. These questions are important because they affect the interpretation of BSE images of cement-based materials.

6. Conclusions

Scanning electron microscopy in backscattered electron mode, within its limits, can be an invaluable tool for cement and concrete research. The key lies in having the right sample preparation technique and a good understanding of the principles of electron microscopy, signal generation and image formation, so as to avoid misunderstanding and misinterpretation of the BSE images.

For the examination of cement-based materials by BSE imaging, it is critical to ensure that the observation plane is saturated with an epoxy resin. The resin stabilises the microstructure and minimises damage during grinding and polishing, and also provides contrast between the pore and solid phase. However, conventional epoxy impregnation under vacuum can only achieve a very shallow penetration depth. Thus, extreme care must be followed so that the sample is not ground beyond the epoxy penetration depth.

In this paper, a modified epoxy impregnation method is proposed. This method can achieve a deeper epoxy penetration, in the order of several millimetres, compared to hundreds of microns in the conventional technique. The deeper epoxy penetration gives more allowance for grinding and polishing, assuring that the finished surface remains saturated with epoxy.

BSE imaging on mortars that were prepared using conventional vacuum impregnation showed that hydrated cement paste consists of large patches of dense almost non-porous and porous regions that occur irregularly in the ITZ and bulk regions. The boundary between patches is very distinct and sharp. When the same samples were re-impregnated using the proposed method and re-polished, it was observed that all the dense patches disappeared, replaced by a paste that showed many capillary pores and hollow shells previously not seen. We conclude that the patchy microstructure is an artefact of sample preparation; the dense patch is a false impression caused by pastes that have been ground beyond the epoxy intrusion depth.

This paper has shown that an incorrect sample preparation technique can give a very misleading picture of cement paste microstructure and can have a major influence on qualitative assessment or quantitative measurements via image analysis of BSE images. Unfortunately, the true extent of this problem is yet to be known. Concrete and cement-based materials are naturally heterogeneous materials, with the heterogeneity occurring across different scales, but previously reported occurrence of broad patches of dense and porous regions is almost certainly an artefact of sample preparation and is not a true feature. Thus, the conclusion that the overlapping of these porous patches could lead to percolative effects should be viewed with caution. However, we emphasise that the results presented in this paper do not, in anyway, validate or provide additional support for the conventional ITZ model or the NIST hard core/soft shell model.

Acknowledgements

HSW would like to acknowledge the financial assistance provided by the Universities UK, via the Overseas Research

Students Awards Scheme. We thank Mr. R.A. Baxter for his help with the laboratory work.

References

- [1] S. Diamond, Percolation due to overlapping ITZs in laboratory mortars? A microstructural evaluation, *Cem. Concr. Res.* 33 (7) (2003) 949–955.
- [2] S. Diamond, The patchy structure of cement paste in conventional concretes, 'Concrete Science and Engineering: a Tribute to Arnon Bentur', RILEM Proc. PRO 36, RILEM Publications S.A.R.L., Paris, 2004, 85–94.
- [3] S. Diamond, The microstructure of cement paste and concrete – a visual primer, *Cem. Concr. Compos.* 26 (8) (2004) 919–933.
- [4] S. Diamond, The patch microstructure in concrete: effect of mixing time, *Cem. Concr. Compos.* 35 (5) (2005) 1014–1016.
- [5] D.N. Winslow, M.N. Cohen, D.P. Bentz, K.A. Snyder, E.J. Garboczi, Percolation and pore structure in mortars and concrete, *Cem. Concr. Res.* 24 (1994) 25–37.
- [6] D.P. Bentz, E.J. Garboczi Computer modelling of interfacial transition zone: microstructure and properties, in: M.G. Alexander et al. (Eds.), *Engineering and Transport Properties of the Interfacial Transition Zone in Cementitious Composites*, RILEM Report, 20, RILEM Publications SARL, Paris, 1999, pp. 349–385.
- [7] K.O. Kjellsen, A. Monsøy, K. Isachsen, R.J. Detwiler, Preparation of flat-polished specimens for SEM-backscattered electron imaging and X-ray microanalysis – importance of epoxy impregnation, *Cem. Concr. Res.* 33 (2003) 611–616.
- [8] D.A. St John, A.W. Pole, I. Sims, *Concrete Petrography: a Handbook of Investigative Techniques*, Arnold, London, 1998, 474 pp.
- [9] P.E. Stutzman, J.R. Clifton, *Specimen Preparation for Scanning Electron Microscopy*, 21st International Conferences on Cement Microscopy, Las Vegas, Nevada, 1999, 10–22.
- [10] S. Diamond, J. Huang, Interfacial transition zone: reality or myth? in: A. Katz, A. Bentur, M. Alexander, G. Arliguie (Eds.), *Proc. RILEM 2nd Int. Conf. On the Interfacial Transition Zone in Cementitious Composites*, RILEM Publications SARL, Paris, 1998, 35, 1–40.
- [11] S. Diamond, J. Huang, The ITZ of concrete – a different view based on image analysis and SEM observations, *Cem. Concr. Compos.* 23 (2001) 179–188.